Separation Science and Technology
Publication details, including instructions for authors and subscription information:
http://www.informaworld.com/smpp/title~content=t713708471

A Study on the Solute Separation and the Pore Size Distribution of a Montmorillonite Membrane

M. Ishiguro[a]; T. Matsuura[b]; C. Detellier[c]
[a] NATIONAL RESEARCH INSTITUTE OF AGRICULTURAL ENGINEERING, IBARAKI, JAPAN [b] INDUSTRIAL MEMBRANE RESEARCH INSTITUTE DEPARTMENT OF CHEMICAL ENGINEERING, UNIVERSITY OF OTTAWA, OTTAWA, KIN, CANADA [c] DEPARTMENT OF CHEMISTRY, UNIVERSITY OF OTTAWA, OTTAWA, KIN, CANADA

To cite this Article Ishiguro, M. , Matsuura, T. and Detellier, C.(1996) 'A Study on the Solute Separation and the Pore Size Distribution of a Montmorillonite Membrane', Separation Science and Technology, 31: 4, 545 — 556
To link to this Article: DOI: 10.1080/01496399608002216
URL: http://dx.doi.org/10.1080/01496399608002216

SEPARATION SCIENCE AND TECHNOLOGY, 31(4), pp. 545–556, 1996

A Study on the Solute Separation and the Pore Size Distribution of a Montmorillonite Membrane

M. ISHIGURO
NATIONAL RESEARCH INSTITUTE OF AGRICULTURAL ENGINEERING
2-1-2 KANNONDAI, TSUKUBA, IBARAKI, 305, JAPAN

T. MATSUURA
INDUSTRIAL MEMBRANE RESEARCH INSTITUTE
DEPARTMENT OF CHEMICAL ENGINEERING
UNIVERSITY OF OTTAWA
OTTAWA K1N 6N5, CANADA

C. DETELLIER
DEPARTMENT OF CHEMISTRY
UNIVERSITY OF OTTAWA
OTTAWA K1N 6N5, CANADA

ABSTRACT

A montmorillonite membrane with a thickness of 0.5 mm was prepared, and reverse osmosis experiments were conducted for various inorganic and organic solutes of different sizes under an operating pressure of 3 MPa. The mean pore size and pore size distribution were determined by a log-normal probability plot between the solute separation and the Einstein–Stokes radius of the solute molecules for which reverse osmosis and ultrafiltration performance was investigated. The relationships between the pore size and the pore size distribution and the structure of montmorillonite are discussed. A comparison is also made between the pore size and the thickness of the electrical double layer.

INTRODUCTION

As the scope of membrane separation technology broadens, resistance against heat, chemicals, and corrosion becomes an increasingly desired feature of the membrane material (1). Unfortunately, polymeric materials from which most commercial membranes are currently produced do not necessarily meet these requirements. For this reason, various inorganic materials have been investigated for the manufacture separation membranes.

It has long been known that montmorillonite, a clay material of the smectite family, exhibits salt rejection when a layer of it is used as a membrane in reverse osmosis experiments (2–11). However, its applicability to membrane separation technology has not yet been fully developed.

The building elements of the semectites are two-dimensional arrays of silicon-oxygen tetrahedra and aluminum or magnesium oxygen-hydroxyl octahedra. The interlayer distance between the repeat layers is determined by *d*001 spacing as measured by x-ray powder diffraction. Due to substitution of the Al atoms in the octahedra and the Si atoms in the tetrahedra by lower valence atoms, a negative charge results in the layer. This negative charge is compensated for by adsorbed or intercalated exchangeable cations such as sodium and calcium.

Recognizing montmorillonite's unique structure, performance testing was carried out for the separation of gaseous mixtures either by gas chromatography (12, 13) or by membranes in which montmorillonite was incorporated in a silicone rubber film (14). Montmorillonite was also incorporated in alumina membranes prepared by the sol–gel method for the separation of hydrocarbon mixtures (15).

In earlier investigations we tested the separation of nonionized organic solutes and amino acids and found that the montmorillonite membrane can fractionate the mixtures of a nonionized organic solute and an electrolyte solute much more effectively than synthetic polymeric membranes with charges (16).

The objective of this work is to test the montmorillonite membrane for the separation of macromolecules from water by ultrafiltration. Another objective is to establish the average pore size and the pore size distribution from a plot of solute separation versus the Einstein–Stokes radius. An attempt is also made to compare the pore size distribution so obtained with the structural characteristics of the montmorillonite material.

EXPERIMENTAL

Materials

The crude montmorillonite (SWy-1, Wyoming bentonite) was obtained from the Clay Source Repository, University of Missouri. It was purified by sedimentation, and the homoionic sodium form was obtained according to a method described elsewhere (17). The cation-exchange capacity and the surface area of the purified montmorillonite were 0.83 $meq \cdot g^{-1}$ and 646 $m^2 \cdot g^{-1}$, respectively (17). The density of clay determined by using a Multivolume Pycnometer 1305 (Micrometrics) was 2.72 $g \cdot cm^{-3}$. It was checked by particle size analysis that more than 90% of the sample was <0.2 μm equivalent spherical diameter (e.s.d.). All other chemicals were of reagent grade and used without further purification.

Separation Experiments

The permeation cell and the equipment used for the separation experiments are shown schematically in Fig. 1. The procedure of clay membrane preparation is described thoroughly in our previous work (16). Briefly, the purified clay in sodium form was sandwiched between two millipore filters (pore diameter = 0.1 μm) and placed in the permeation cell. The thickness of the clay membrane was 0.5 mm with a water content of 59 vol%.

The separation experiments were carried out at an operating pressure of 3 MPa gauge and a temperature of 22°C. The feed concentrations of

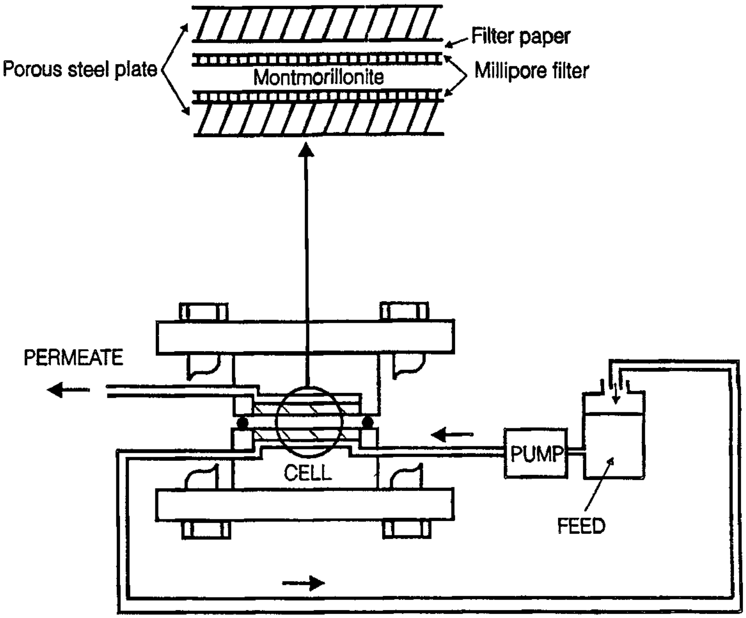

FIG. 1 Schematic diagram of the permeation cell and the experimental apparatus.

sodium chloride and amino acid solutes were 1 mmol/L. The feed concentrations of the other organic solutes were 100 carbon ppm. The solutes used in this work and their pertinent physical properties are listed in Table 1. For each solute separation experiment, the permeation rate, g/h, and the solute separation, f, defined as

$$f = \frac{\text{(feed solute concentration)} - \text{(permeate solute concentration)}}{\text{(feed solute concentration)}} \tag{1}$$

TABLE 1
Solutes and Their Pertinent Physicochemical Data

Solute	Molecular weight (dalton)	Einstein–Stokes radius × 10^{10} (m)	Days[a]
Acetone	58.1	1.91	13
Methyl ethyl ketone	72.1	1.92	16
n-Hexanol	102.2	1.97	34
Phenol	94.1	2.1	31
Glycerol	92.1	2.3	28
n-Butanol	74.1	2.33	19
Glucose	180.2	3.66	36
Sucrose	342.3	4.67	41
Raffinose	504.4	5.56	133
β-Cyclodextrin	1,135	8.57	136
Dextran 9,400	9,400	22.8	140
66,300	66,300	56.3	149
480,000	480,000	141	153
Polyethylene glycol 200	200	3.86	38
300	300	4.56	79
400	400	5.16	45
600	600	6.27	49
1,000	1,000	7.89	52
1,500	1,500	9.85	57
2,000	2,000	11.43	60
4,000	4,000	15.34	62
9,000	9,000	28.9	65
20,000	20,000	31.0	69
35,000	35,000	33.1	72
Na^+	22.99	1.83	4
Cl^-	35.45	1.20	4
L-Glutamic acid	147.1	3.47	128
L-Methionine	149.2	3.65	164
L-Lysine	146.2	3.73	86

[a] Days from the start of the series of experiments.

were determined. The sodium chloride concentration was determined conductometrically, whereas the organic solutes concentrations were determined by using a high-temperature Total Organic Carbon analyzer, Rosemont Analytical Inc., DC-190.

THEORETICAL

Sieving Curves Approach

According to the sieving curves approach to characterize the pore size distribution of ultrafiltration membranes, the sieving coefficient ($\theta = 1 - f$) is given as a function of the Einstein–Stokes radius (ESR) as

$$\theta = 1 - \mathrm{erf}(\tau) \tag{2}$$

where

$$\tau = \log(a/\mathbf{a})/\log \sigma_a \tag{3}$$

a is the Einstein–Stokes radius, **a** is the ESR of the "mean" macromolecule, and σ_a is the geometric standard deviation about the mean ESR. A linear relationship between θ and a is expected on log-normal probability plot according to Eqs. (2) and (3). **a** is obtained on the latter plot as an ESR corresponding to $\theta = 0.5$. σ_a can be determined from the ratio of a at $\theta = 0.159$ and a at $\theta = 0.5$ (18).

This approach is based on the following assumptions.

1. The Stokes–Einstein radius can represent the size of a solute molecule.
2. The size and the shape of a solute molecule do not depend on whether the solute is in the bulk solution or in the membrane pore.
3. The transport of a solute molecule is not affected by the interaction force working between the solute and the membrane.
4. Sieving is the only mechanism for solute separation.

None of the above conditions can, in reality, be satisfied. Nevertheless, this approach will be used in the following because of its simplicity.

Einstein–Stokes Radius of Solutes

The Einstein–Stokes radius (ESR), a (m), is defined by the Stokes–Einstein equation

$$a = kT/6\pi\eta D \tag{4}$$

where k is the Boltzmann constant (J/K), T is the absolute temperature (T), η is the solvent viscosity (Pa·s), and D is the diffusivity (m^2/s).

The ESR values for the solutes used in this work are listed in Table 1 and were obtained in the following way. Starting from the smallest ESR, acetone to sucrose are from Sourirajan and Matsuura (19). Those of polyethylene glycol (PEG) from 600 to 4000 are also from Sourirajan and Matsuura (19). ESR values for cyclodextrin and dextrans were calculated by using the following relationship between ESR and the molecular weight (20, 21).

$$a = 0.33M^{0.643} \tag{5}$$

The diffusivity data for raffinose, Na^+, and Cl^- were found in the literature (22) and used in Eq. (4). The diffusivity data for amino acids were from Matsuura and Sourirajan (23) and also used in Eq. (4). In order to obtain ESR values for PEG solutes other than those for which ESR values were already known, diffusivity data were first calculated by the following equation (24–26)

$$D = 1.2 \times 10^7 \, kT/\{\eta(M \, \eta_I)^{1/3}\} \tag{6}$$

where D is the diffusivity (m^2/s), k is the Boltzmann constant (J/K), η is the viscosity of water (Pa·s), M is the molecular weight (kg/mol), and η_I is the intrinsic viscosity of an aqueous solution of PEG solute (m^3/kg). Then, Eq. (4) was used to calculate ESR. η_I is given in Ref. 25.

RESULTS AND DISCUSSION

The log-normal probability relationship between solute separation and ESR is shown in Fig. 2 for various solutes studied in this work. Since separations of acetone, methyl ethyl ketone, and PEG 200 were 0, these solutes could not be plotted on the figure.

Open circles are for the nonionized organic solutes other than PEG. These data were subjected to linear regression analysis, and the solid line is the result. The correlation coefficient was 0.953, indicating a very good fit of the line to the data. The analysis also produced a geometric mean of 33.6×10^{-10} m, ESR corresponding to 50% solute separation, and a geometric standard deviation of 7.35. Applying the same technique, Michaels reported geometric means ranging from 17×10^{-10} to 34×10^{-10} m for membranes including synthetic ultrafiltration membranes and mammalian glomerular membranes. The range for the geometric standard deviations was from 1.2 to 1.7.

It should be noted that the standard deviation of the montmorillonite membrane is four to six times larger than those of membranes studied by Michaels, indicating, according to this approach, a significantly broader pore size distribution of the montmorillonite membrane. The narrower

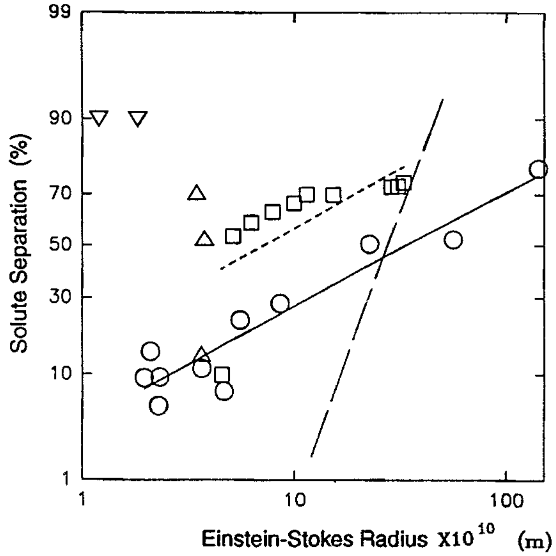

FIG. 2 Log-normal probability plot of solute separation versus Einstein–Stokes radius. (- - - □) Polyethylene glycol, (—— ○) nonionized organic solutes other than polyethylene glycol, (△) amino acids, (▽) Na^+ and Cl^-, (—) Rhone-Poulenc AN 69 dialysis membrane from Ref. 18.

pore size distribution of a synthetic polymeric membrane is visualized in Fig. 2 by a steep broken line that corresponds to a Rhone-Poulenc AN 69 dialysis membrane (18) based on the experimental data of Green et al. (27). This line produced a geometric mean of 27.7×10^{-10} m and a standard deviation of 1.49.

Because of its broad pore size distribution, solute separation of the montmorillonite membrane increased from 25% to only 78% when the molecular wieght of the solute increased almost 1000-fold from 504 (raffinose) to 480,000 (dextran 480,000).

If the molecular weight cutoff (MWC) of a ultrafiltration membrane is defined as the solute molecular weight at which 90% separation is achieved, the MWC of the montmorillonite membrane is well over 500,000. It is surprising that the same montmorillonite membrane showed 90% of sodium chloride separation, as indicated in Fig. 2 by two reverse triangular points corresponding to ionic sizes of Na^+ and Cl^- ions.

Montmorillonite is a member of the smectite family, the building elements of which are two-dimensional arrays of silicon-oxygen tetrahedra and aluminum or magnesium oxygen-hydroxyl octahedra. Because of this two-dimensional nature, a building element of SWy-1 montmorillonite is a flat sheet having a thickness of 7×10^{-10} m and a side length of 80×10^{-10} to 250×10^{-10} m.

Furthermore, due to substitution of the Al atoms in the octahedra and the Si atoms in the tetrahedra by lower valence atoms, a negative charge results in the layer. The negative charge is compensated for by adsorbed or intercalated exchangeable cations such as sodium and calcium.

A simple model of the montmorillonite structure is a uniformly laminated sheet structure (28) in which a layer is formed by packing many flat building elements two-dimensionally without leaving space between the building elements. These layers are then laminated one after another, retaining water in the interlayer space. The interlayer distance is controlled by the swelling pressure of water, resulting in a uniform thickness of water.

Assuming the volume of montmorillonite represents that of one flat layer, whereas the volume of water represents that of water in the interlayer space, the distance between two sheet can be calculated by

$$h = 7 \times 10^{-10} \times (\epsilon/1 - \epsilon)$$

where ϵ is the volume fraction of water in wet montmorillonite. Since ϵ is known to be 0.59 in the membrane, h is equal to 10×10^{-10} m.

It is interesting to note that the pore size distribution of the montmorillonite membrane expressed by the log-normal probability relationship covers the range from 4×10^{-10} to over 282×10^{-10} m in diameter, which overlaps the dimension of the montmorillonite building element; i.e., the interlayer water thickness of 10×10^{-10} m as a lower limit and the side length of 80×10^{-10} to 250×10^{-10} m as an upper limit. This suggests that only a part of the building elements are arrayed according to the uniformly laminated sheet structure, and most of them are randomly placed.

The separation of ionic solutes can be explained on the basis of the double layer theory (29). The thickness of the electric double layer can give the approximate size of the pore into which an ionic solute cannot enter because of the overlap of the double layer. Furthermore, the reciprocal of the Debye length κ is considered as a measure of the double-layer thickness (30). κ can be calculated by

$$\kappa^{-1} = \{(\Xi RT)/(2z^2F^2c)\}^{1/2}$$

where Ξ is the dielectric constant (695.4×10^{-12} F/m for water), R is the gas constant (8.314 J/mol·K), z is the valence, F is the Faraday constant (9.648×10^4 C/mol), and c is the concentration (mol/m^3).

Using the above numerical values, κ^{-1} for an ion of valence 1 is calculated to be 100 × 10^{-10} m at a concentration of 1 mol/m^3 (31). If the thickness of two double layers is the diameter of pores from which the ions are excluded, then a pore diameter of 200 × 10^{-10} m allows the rejection of an ion of valence 1. Therefore, it was possible to separate 90% of sodium chloride by the montmorillonite membrane whose pore size ranges from 4 to over 282 × 10^{-10} m. Only the largest pores allowed the passage of the electrolyte solute.

The solute separation data of PEG did not fall on the line drawn by the linear regression fit to the separation data of nonionized organic solutes. A steep increase of solute separation from PEG 200 (0%) to PEG 400 (58.7%) was observed. Then, PEG separations increased only moderately as their ESR increased. The linear regression fit to the PEG separation data was attempted without including PEG 200 data. The correlation coefficient was only 0.684, since the data for PEG 300 differed greatly from that of the rest of PEG solutes. Despite the low correlation coefficient, the result of the linear regression fit is shown as a broken line on Fig. 2, which resulted in a geometric mean of 7.14 × 10^{-10} m and a standard deviation of 6.71. Since the slopes of the solid and the broken lines are close to each other, similar values were obtained for the standard deviation from both lines, confirming the broad pore size distribution of the montmorillonite membrane. However, because the position of the broken line is far above that of the solid line, the geometrical mean obtained from PEG solutes is far smaller than that obtained by other nonionized organic solutes.

The behavior of PEG solutes, which is noticeably different from that of other nonionized organic solutes, can probably be ascribed to the shape of the PEG molecules. Among solute molecules whose molecular weights are more than 500 dalton, only PEGs are straight-chain molecules. Others contain either cyclic components (raffinose and β-cyclodextrin) or are branched (dextrans). The unique separation features of straight-chain macromolecules were reported for synthetic polymeric membranes (32). Interestingly, straight-chain macromolecules permeate through pores of synthetic polymeric membranes more readily than do bulky macromolecules, and this is interpreted as the stretching of chain-like macromolecules in the membrane pore. As a result, MWC obtained by PEC molecules is larger than that obtained by more bulky macromolecules. The separation data obtained for the montmorillonite membrane is opposite to this effect. PEG molecules whose molecular weights are equal to or less than 300 dalton are not considered as straight chain macromolecules and behave more like other nonionized organic molecules.

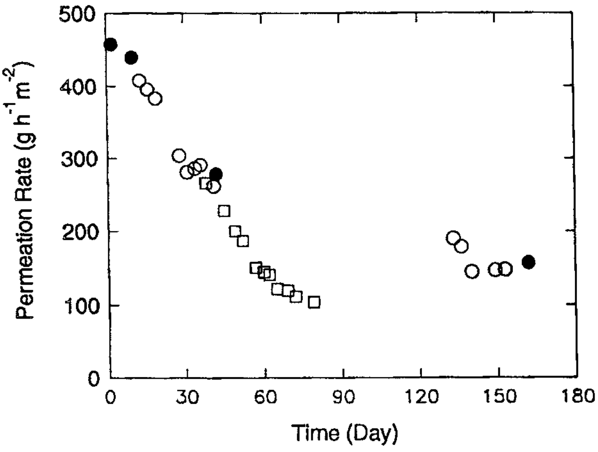

FIG. 3 Permeation rate versus time. (□) Polyethylene glycol, (○) nonionized organic solutes, (●) pure water permeation.

Although the size of three amino acids are similar, separation of L-methionine, which has no net charge, falls on the solute separation and ESR correlation line for the nonionized organic solutes, whereas those of L-glutamic acid and L-lysine, which have net electric charges, are far above the correlation line. This aspect was discussed in our earlier paper more in detail (16).

The permeation rate data corresponding to nonionized organic solutes are shown in Fig. 3. This series of experiments was continued for 164 days without interruption. Starting from acetone solute, whose reverse osmosis experiment was carried out on the 13th day, the day of the experiment is recorded in the last column of Table 1. The pure water permeation data are also given in Fig. 3 as filled circles. The figure shows that the permeation rate decreased gradually from 450 $g \cdot h^{-1} \cdot m^{-2}$ to about 100 $g \cdot h^{-1} \cdot m^{-2}$ from the start of the experiment to the 72nd day when the PEG experiments were completed. This is considered to be due to compaction of the membrane. Amino acids separations were carried out between the 72nd and the 133rd day under pH values higher or lower than neutral. This treatment brought the permeation rate back to 200 $g \cdot h^{-1} \cdot m^{-2}$, after which the permeation rate started to decrease again when raffinose, β-cyclodextrin and dextrans were treated.

CONCLUSIONS

The following conclusions can be drawn from the above experimental results.

1. The mean pore radius of the montmorillonite membrane is in the same range as that of synthetic polymeric ultrafiltration membranes.
2. The monmorillonite membrane has a significantly broader pore size distribution than synthetic polymeric membranes.
3. Small nonionized organic molecules flow through the pores belonging to the upper end of the pore size distribution.
4. Although the pore sizes are those of ultrafiltration membranes, electrolyte solutes can be rejected from the membrane pores because of the thick electrical double layers formed in the pore.

REFERENCES

1. T. Ohtani, "Inorganic Membranes for Separation in Liquid Media," *Maku (Membrane)*, *19*, 155 (1994).
2. J. G. McKelvey and I. H. Milne, "The Flow of Salt Solutions through Compacted Clay," *Clays Clay Miner.*, *9*, 248 (1962).
3. W. D. Kemper and D. E. L. Maasland, "Reduction in Salt Content of Solution on Passing through Thin Films Adjacent to Charged Surfaces," *Soil Sci. Soc. Am., Proc.*, *28*, 318 (1964).
4. G. Jacazio, R. F. Probstein, A. A. Sonin, and D. Yung, "Electrokinetic Salt Rejection in Hyperfiltration through Porous Materials: Theory and Experiment," *J. Phys. Chem.*, *76*, 4015 (1972).
5. Y. K. Kharaka and F. A. F. Berry, "Simultaneous Flow of Water and Solutes through Geological Membranes: I. Experimental Investigation," *Geochim. Cosmochim. Acta*, *37*, 2577 (1973).
6. D. E. Elrick, D. E. Smiles, N. Baumgartner, and P. H. Groenevelt, "Coupling Phenomena in Saturated Homo-ionic Montmorillonite: I. Experimental," *Soil Sci. Soc. Am. J.*, *40*, 490 (1976).
7. P. F. Rolfe and L. A. G. Aylmore, "Water and Salt Flow through Compacted Clays: II. Electrokinetics and Salt Sieving," *J. Colloid Interface Sci.*, *79*, 301 (1981).
8. W. M. Benzel and D. L. Graf, "Studies of Smectite Membrane Behavior: Importance of Layer Thickness and Fabric in Experiments at 20°C," *Geochim. Cosmochim. Acta*, *48*, 1769 (1984).
9. S. J. Fritz, "Ideality of Clay Membranes in Osmotic Processes: A Review," *Clays Clay Miner.*, *34*, 214 (1986).
10. I. Demir, "Studies of Smectite Membrane Behavior: Electrokinetic, Osmotic, and Isotopic Fractionation Processes at Elevated Pressures," *Geochim. Cosmochim. Acta*, *52*, 727 (1988).
11. S. Iwata, "Flow of Solutions through Clay Layers," in *Soil–Water Interactions* (S. Iwata, T. Tabuchi, and B. P. Warkentin, Eds.), Dekker, New York, 1988, pp. 167–193.
12. H. Lao, S. Latieule, and C. Detellier, "Molecular Recognition in Microporous Organo-

Minerals. Shape-Specific Interactions of Carbon Dioxide in Functionalized Organo-Montmorillonite Microcavities," *Chem. Mater.*, *3*, 1009 (1991).

13. H. Lao and C. Detellier, "Gas Chromatographic Separation of Linear Hydrocarbons on Microporous Organo-Smectites," *Clays Clay Miner.*, *42*, 477 (1994).
14. H. Lao, "Novel Microporous Organo-Clay Materials and Organo-Clay Polymeric Composite Membranes," Ph.D. Thesis, University of Ottawa, 1993.
15. H. Lao, C. Detellier, T. Matsuura, and A. Y. Tremblay, "Microporous Inorganic Membranes: Preparation by the Sol-Gel Process and Characterization of Unsupported Composite Membranes of Alumina and Polyammonium Pillared Montmorillonite," *J. Mater. Sci. Lett.*, *13*, 895–897 (1994).
16. M. Ishiguro, T. Matsuura, and C. Detellier, "Reverse Osmosis Separation for a Montmorillonite Membrane," *J. Membr. Sci.*, in press (1995).
17. L. Mercier and C. Detellier, "Intercalation of Tetraalkylammonium Cations into Smectites and Its Application to Internal Surface Area Measurements," *Clays Clay Miner.*, *42*, 71 (1994).
18. A. S. Michaels, "Analysis and Prediction of Sieving Curves for Ultrafiltration Membranes: A Universal Correlation?," *Sep. Sci. Technol.*, *15*, 1305 (1980).
19. S. Sourirajan and T. Matsuura, *Reverse Osmosis/Ultrafiltration Process Principles*, National Research Council, Ottawa, Canada, 1985.
20. K. Granath, *J. Colloid Sci.*, *13*, 308 (1958).
21. K. Granath and K. Kvist, *J. Chromatogr.*, *28*, 69 (1967).
22. D. R. Lide (Ed.), *CRC Handbook of Chemistry and Physics*, 73rd ed., CRC Press, Boca Raton, Florida, 1992, pp. 5–111 and 6–175.
23. T. Matsuura and S. Sourirajan, "Reverse Osmosis Separation of Amino Acids in Aqueous Solutions Using Porous Cellulose Acetate Membranes," *J. Appl. Polym. Sci.*, *18*, 3593 (1974).
24. F.-H. Hsieh, T. Matsuura, and S. Sourirajan, "Reverse Osmosis Separations of Polyethylene Glycols in Dilute Aqueous Solutions Using Porous Cellulose Acetate Membranes," *Ibid.*, *23*, 561 (1978).
25. F.-H. Hsieh, T. Matsuura, and S. Sourirajan, "Analysis of Osmosis Data for System Polyethylene Glycol–Water–Cellulose Acetate Membrane at Low Operating Pressures," *Ind. Eng. Chem., Process Des. Dev.*, *18*, 414 (1979).
26. L. Mandelkern and P. J. Flory, *J. Chem. Phys.*, *20*, 212 (1952).
27. D. M. Green, G. D. Antwiler, J. W. Mancrief, J. F. Decherd, and R. P. Popovich, *Trans. Am. Soc. Artif. Intern. Organs*, *22*, 627 (1976).
28. J. D. Sherwood, "Ionic Motion in a Compacting Filtercake," *Proc. R. Soc. London, Ser. A: Math. Phys. Sci.*, *437*, 489 (1992).
29. P. Neogi and E. Ruckenstein, "Viscoelectric Effects in Reverse Osmosis," *J. Colloid Interface Sci.*, *79*, 159 (1981).
30. E. J. W. Verwey and J. T. G. Overbeek, *Theory of the Stability of Lyphobic Colloids*, Elsevier, New York, 1948.
31. S. Iwata, "Interaction between Soil Particles and Soil-Solution," in *Soil–Water Interactions* (S. Iwata, T. Tabuchi, and B. P. Warkentin, Eds.), Dekker, New York, 1988, pp. 63–130.
32. W. Eykamp, "Microfiltration and Ultrafiltration," in *Membrane Separations Technology—Principles and Applications* (R. D. Noble and S. A. Stern, Eds.), Elsevier, New York, 1995, pp. 1–43.

Received by editor June 5, 1995